

Photochemistry of the Triangular Clusters $\text{Os}_3(\text{CO})_{10}(\alpha\text{-diimine})$: Homolysis of an Os–Os Bond and Solvent-Dependent Formation of Biradicals and Zwitterions

Jos Nijhoff, Maarten J. Bakker, František Hartl, and Derk J. Stufkens*

Anorganisch Chemisch Laboratorium, J.H. van 't Hoff Research Institute, Universiteit van Amsterdam, Nieuwe Achtergracht 166, 1018 WV Amsterdam, The Netherlands

Wen-Fu Fu and Rudi van Eldik

Institut für Anorganische Chemie, Universität Erlangen-Nürnberg, Egerlandstrasse 1, 91058 Erlangen, Germany

Received June 12, 1997

Several clusters $\text{Os}_3(\text{CO})_{10}(\alpha\text{-diimine})$ ($\alpha\text{-diimine}$ = pyridine-2-carbaldehyde *N*-*R*-imine or 1,4-di-*R*-1,4-diazabutadiene) were synthesized and studied with respect to their spectroscopic and photochemical properties. According to the resonance Raman spectra the visible absorption band of these clusters belongs to electronic transitions having Os-to- α -diimine charge transfer (MLCT) character with a variable degree of π -delocalization within the Os(α -diimine) moiety. Upon irradiation into these transitions zwitterions $^-\text{Os}(\text{CO})_4\text{--Os}(\text{CO})_4\text{--Os}^+(\text{CO})_2(\alpha\text{-diimine})$ (S)(CO)₂(α -diimine) are formed in coordinating solvents (S) and biradicals $^{\bullet}\text{Os}(\text{CO})_4\text{--Os}(\text{CO})_4\text{--Os}^+(\text{CO})_2(\alpha\text{-diimine}^{\bullet-})$ in noncoordinating solvents and in THF at ambient temperature. The zwitterions live seconds in nitrile solvents and minutes in pyridine, and they largely regenerate the parent clusters. Quantum yields of zwitterion formation are wavelength independent and range from 10^{-2} to 3×10^{-2} with an activation energy varying from 440 to 720 cm^{-1} . For one of the clusters the quantum yield of zwitterion formation in pyridine was studied in dependence of applied pressure. The activation volume $\Delta V^\ddagger = +7.0 \pm 0.5 \text{ cm}^3 \text{ mol}^{-1}$ derived from these measurements indicates that the effect of bond cleavage is partially offset by coordination of the solvent. In apolar solvents biradicals are formed instead of zwitterions, which could be detected with nanosecond time-resolved absorption spectroscopy, while their adducts with nitrosodurene were observed with EPR spectroscopy. Their lifetimes vary from 5 ns to 1 μs depending on the solvent and the α -diimine. The biradicals transform into zwitterions in the presence of a Lewis base. In addition, they produce with low efficiency an isomeric product in which the α -diimine bridges between two Os atoms. The formation of very similar photoproducts (biradicals, α -diimine-bridged isomeric products, charge-separated species) as in the case of binuclear metal–metal-bonded complexes such as $(\text{CO})_5\text{MnMn}(\text{CO})_3(\alpha\text{-diimine})$ points to the occurrence of a primary photoprocess in which an Os–Os bond is broken homolytically. This reaction most likely occurs from a reactive $^3\sigma\pi^*$ state after surface crossing from the unreactive but optically accessible MLCT states.

Introduction

Light-induced homolysis reactions of α -diimine complexes, in which the α -diimine represents e.g. 2,2'-bipyridine (bpy), have been observed for a great variety of metal–metal-bonded compounds. Examples are $L_n\text{MRe}(\text{CO})_3(\alpha\text{-diimine})$ ($L_n\text{M} = (\text{CO})_5\text{Mn}, (\text{CO})_5\text{Re}, (\text{CO})_4\text{Co}, \text{Cp}(\text{CO})_2\text{Fe}, \text{Ph}_3\text{Sn}$),^{1–15} $(\text{CO})_5\text{MnMn}(\text{CO})_3(\alpha\text{-diimine})$,^{6,12} $L_n\text{MRu}(\text{Me})(\text{CO})_2(\alpha\text{-diimine})$

($L_n\text{M} = (\text{CO})_5\text{Mn}, (\text{CO})_5\text{Re}, (\text{CO})_4\text{Co}, \text{SnPh}_3, \text{PbPh}_3$),^{16,17} and $\text{Ru}(\text{SnPh}_3)_2(\text{CO})_2(\alpha\text{-diimine})$.¹⁷ A similar reaction occurs for the mononuclear metal–alkyl complexes $\text{M}(\text{R})(\text{CO})_3(\alpha\text{-diimine})$ ($\text{M} = \text{Mn}, \text{Re}$),^{18–22} $\text{Ru}(\text{X})(\text{R})(\text{CO})_2(\alpha\text{-diimine})$ ($\text{X} = \text{halide}$),^{22,23} $\text{Ir}(\text{R})(\text{CO})(\text{PAR}_3)_2(\text{mnt})$,²⁴ $\text{Pt}(\text{Me})_4(\alpha\text{-diimine})$,²⁵ and

* To whom correspondence should be addressed.

- (1) Stufkens, D. J. *Comments Inorg. Chem.* **1992**, *13*, 359.
- (2) Morse, D. L.; Wrighton, M. S. *J. Am. Chem. Soc.* **1976**, *98*, 3931.
- (3) Luong, J. C.; Faltynek, R. A.; Wrighton, M. S. *J. Am. Chem. Soc.* **1980**, *102*, 7892.
- (4) Luong, J. C.; Faltynek, R. A.; Wrighton, M. S. *J. Am. Chem. Soc.* **1979**, *101*, 1597.
- (5) Stufkens, D. J. *Coord. Chem. Rev.* **1990**, *104*, 39.
- (6) Kokkes, M. W.; Stufkens, D. J.; Oskam, A. *Inorg. Chem.* **1985**, *24*, 4411.
- (7) Kokkes, M. W.; Stufkens, D. J.; Oskam, A. *Inorg. Chem.* **1985**, *24*, 2934.
- (8) Kokkes, M. W.; de Lange, W. G. J.; Stufkens, D. J.; Oskam, A. *J. Organomet. Chem.* **1985**, *294*, 59.

- (9) Andréa, R. R.; de Lange, W. G. J.; Stufkens, D. J.; Oskam, A. *Inorg. Chem.* **1989**, *28*, 318.
- (10) van Dijk, H. K.; Stufkens, D. J.; Oskam, A. *Inorg. Chem.* **1989**, *28*, 75.
- (11) Servaas, P. C.; Stor, G. J.; Stufkens, D. J.; Oskam, A. *Inorg. Chim. Acta* **1990**, *178*, 185.
- (12) van der Graaf, T.; Stufkens, D. J.; Oskam, A.; Goubitz, K. *Inorg. Chem.* **1991**, *30*, 599.
- (13) van der Graaf, T.; van Rooy, A.; Stufkens, D. J.; Oskam, A. *Inorg. Chim. Acta* **1991**, *187*, 133.
- (14) van Outersterp, J. W. M.; Stufkens, D. J.; Vlček, A., Jr. *Inorg. Chem.* **1995**, *34*, 5183.
- (15) Rossenaar, B. D.; Lindsay, E.; Stufkens, D. J.; Vlček, A., Jr. *Inorg. Chim. Acta* **1996**, *250*, 5.
- (16) Nieuwenhuis, H. A.; van Loon, A.; Moraal, M. A.; Stufkens, D. J.; Oskam, A.; Goubitz, K. *J. Organomet. Chem.* **1995**, *492*, 165.
- (17) Aarnts, M. P.; Stufkens, D. J.; Vlček, A., Jr. *Inorg. Chim. Acta* **1997**, *266*, 37.

$\text{Zn(R)}_2(\alpha\text{-diimine})^{26}$ and even for the metal–halide complexes $\text{mer-Mn(X)(CO)}_3(\alpha\text{-diimine})$ ($\text{X} = \text{halide}$).²⁷

These homolysis reactions are assumed to occur from a reactive $^3\sigma\pi^*$ state in which σ represents the high-lying metal–metal, metal–alkyl, or metal–halide σ -bonding orbital, and π^* the lowest unoccupied orbital of the α -diimine (or *mnt*) ligand. Quite recently, the $^3\sigma\pi^*$ state of several of these complexes has been characterized by nanosecond time-resolved absorption, emission, and infrared spectroscopy,^{20,21,28} while the alkyl radicals, produced by photolysis of the complexes $\text{Re(R)(CO)}_3(\alpha\text{-diimine})$ and $\text{Ru(X)(R)(CO)}_2(\alpha\text{-diimine})$, were detected with nanosecond time-resolved FT-EPR spectroscopy.²²

The fate of the metal radicals has been studied in most detail for the metal–metal-bonded complexes $(\text{CO})_5\text{MnMn(CO)}_3(\alpha\text{-diimine})$. In noncoordinating, nonviscous solvents the $^*\text{Mn(CO)}_5$ and $\text{Mn(CO)}_3(\alpha\text{-diimine})^*$ radicals diffuse from the solvent cage and dimerize.¹² In coordinating solvents or in the presence of an N- or P-donor ligand, these complexes photodisproportionate into Mn(CO)_5^- and $\text{Mn(CO)}_3(\text{L})(\alpha\text{-diimine})^+$ ($\text{L} = \text{N-}$ or P-donor ligand).^{8,29} Just as for the unsubstituted metal–metal-bonded complexes $\text{Mn}_2(\text{CO})_{10}$, $\text{Cp}_2\text{Mo}_2(\text{CO})_6$, and $\text{Cp}_2\text{Fe}_2(\text{CO})_4$,³⁰ these photodisproportionations proceed via homolysis of the metal–metal bond, adduct formation with L, and electron transfer. In weakly coordinating solvents such as THF the clusters show a temperature-dependent behavior. At room temperature the $^*\text{Mn(CO)}_5$ and $\text{Mn(CO)}_3(\alpha\text{-diimine})^*$ radicals again dimerize, while at temperatures below 200 K the latter radicals take up a solvent molecule and transfer an electron to give the disproportionation products Mn(CO)_5^- and $\text{Mn(CO)}_3(\text{THF})(\alpha\text{-diimine})^+$.²⁹

Apart from these dimerization and disproportionation reactions, the radicals show yet another reaction when the complexes are irradiated in a viscous medium such as paraffin.¹² In such a solvent the radicals stay together since they cannot escape from the solvent cage. Provided the α -diimine contains a reactive imine bond as in the case of R-PyCa or R-DAB (see Figure 1), a radical coupling reaction occurs with formation of free CO and a ligand-bridged photoproduct (Scheme 1).¹²

The reactions, summarized in Scheme 1, prompted us to extend our investigations to triangular clusters of the type $\text{Os}_3(\text{CO})_{10}(\alpha\text{-diimine})$. If these clusters undergo a similar photo-

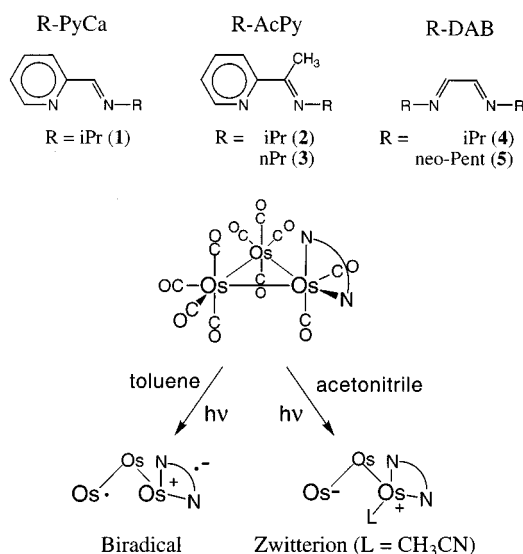
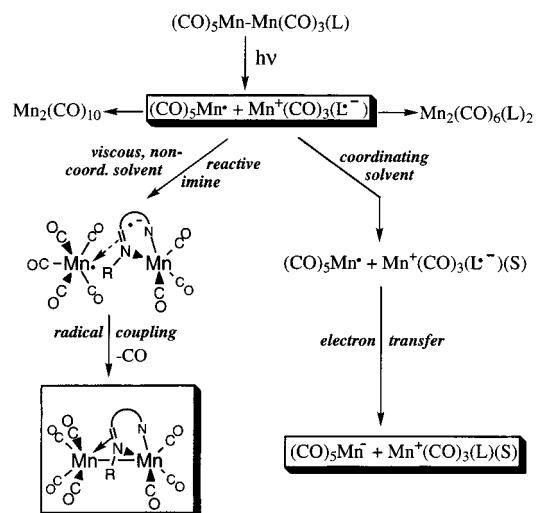


Figure 1. Schematic structures of the $\text{Os}_3(\text{CO})_{10}(\alpha\text{-diimine})$ clusters, of their zwitterions and biradicals, and of the α -diimine ligands used: R-PyCa = pyridine-2-carbaldehyde *N*-alkylimine; R-AcPy = 2-acetylpyridine *N*-alkylimine; R-DAB = *N,N'*-dialkyl-1,4-diaza-1,3-butadiene.

Scheme 1. Photochemical Reactions of the Binuclear Complexes $(\text{CO})_5\text{MnMn(CO)}_3(\text{L})$ in Various Media ($\text{L} = \alpha\text{-Diimine}$)



induced homolysis reaction, they will produce *biradicals*. By analogy with the above binuclear systems, these biradicals may regenerate the parent cluster, transform into a ligand-bridged species in the case of α -diimine = R-PyCa and R-DAB, or undergo an intramolecular electron-transfer reaction in a coordinating solvent with formation of *zwitterions*. Our first investigations in this field were concerned with trisium clusters containing 2,2'-bipyridine and other aromatic α -diimines and showed the formation of zwitterions of the type $^-\text{Os}(\text{CO})_4-\text{Os}^+(\text{S})(\text{CO})_2(\alpha\text{-diimine})$ in acetonitrile and pyridine (S).³¹ There was no evidence of biradical formation in any solvent, and the mechanism of the zwitterion formation remained unclear. This lack of mechanistic information inspired us to study in more detail the zwitterion formation and to search for the formation of biradicals under any circumstances. The mechanism of the zwitterion formation was investigated by determining the quantum yield of one of these reactions at

- (18) Rossenaar, B. D.; Stufkens, D. J.; Oskam, A.; Fraanje, J.; Goubitz, K. *Inorg. Chim. Acta* **1996**, *247*, 215.
 (19) Rossenaar, B. D.; Kleverlaan, C. J.; van de Ven, M. C. E.; Stufkens, D. J.; Oskam, A.; Fraanje, J.; Goubitz, K. *J. Organomet. Chem.* **1995**, *493*, 153.
 (20) Rossenaar, B. D.; George, M. W.; Johnson, F. P. A.; Stufkens, D. J.; Turner, J. J.; Vlček, A., Jr. *J. Am. Chem. Soc.* **1995**, *117*, 11582.
 (21) Rossenaar, B. D.; Kleverlaan, C. J.; van de Ven, M. C. E.; Stufkens, D. J.; Vlček, A., Jr. *Chem. Eur. J.* **1996**, *2*, 228.
 (22) Kleverlaan, C. J.; Martino, D.; van Willigen, H.; Stufkens, D. J.; Oskam, A. *J. Phys. Chem.* **1996**, *100*, 18607.
 (23) Nieuwenhuis, H. A.; van de Ven, M. C. E.; Stufkens, D. J.; Oskam, A.; Goubitz, K. *Organometallics* **1995**, *14*, 780.
 (24) Bradley, P.; Suardi, G.; Zipp, A. P.; Eisenberg, R. *J. Am. Chem. Soc.* **1994**, *116*, 2859.
 (25) Hux, J. E.; Puddephat, R. J. *J. Organomet. Chem.* **1992**, *437*, 251.
 (26) Kaupp, K.; Stoll, H.; Preuss, H.; Kaim, W.; Stahl, T.; van Koten, G.; Wissing, E.; Smeets, W. J.; Spek, A. L. *J. Am. Chem. Soc.* **1991**, *113*, 5606.
 (27) Stor, G. J.; Morrison, S. L.; Stufkens, D. J.; Oskam, A. *Organometallics* **1994**, *13*, 2641.
 (28) Aarnts, M. P.; Stufkens, D. J.; Wilms, M. P.; Baerends, E. J.; Vlček, A., Jr.; Clark, I. P.; George, M. W.; Turner, J. J. *Chem. Eur. J.* **1996**, *2*, 1556.
 (29) van der Graaf, T.; Hofstra, R. M. J.; Schilder, P. G. M.; Rijkhoff, M.; Stufkens, D. J.; van der Linden, J. G. M. *Organometallics* **1991**, *10*, 3668.
 (30) Tyler, D. R. In *Organometallic Radical Processes*; 22nd ed.; W. C. Troglor, Ed.; Elsevier: Amsterdam, 1990; p 338 and references therein.

- (31) van Outersterp, J. W. M.; Garriga Oostenbrink, M. T.; Nieuwenhuis, H. A.; Stufkens, D. J.; Hartl, F. *Inorg. Chem.* **1995**, *34*, 6312.

different pressures. The formation of biradicals was established with EPR and with nanosecond transient absorption spectroscopy. In addition, several crucial experiments were performed to follow the conversion of biradicals into zwitterions. The results of this study will be discussed in the light of the photoreactions of the above Mn complexes. The schematic structures of the α-diimine ligands used, and of the clusters and their zwitterionic and biradical products, are depicted in Figure 1.

Experimental Section

Materials and Preparations. Os₃(CO)₁₂ (ABCR), 2-pyridinecarboxaldehyde, 2-acetylpyridine, glyoxal, (3-(dimethylamino)propyl)amine, *n*-propylamine, and isopropylamine (Janssen) were used as purchased. Solvents of analytical (acetonitrile, pyridine, 2-picoline, and THF) or spectroscopic grade (toluene) quality were dried over sodium wire (THF, toluene) or CaH₂ (acetonitrile, pyridine, 2-picoline) and freshly distilled under nitrogen. 2-Picoline, pyridine, acetonitrile, and butyronitrile were stored on molecular sieves. The ligands R-PyCa,^{32,33} R-AcPy (2-acetylpyridine *N*-alkylimine),³⁴ and R-DAB³⁵ and the clusters Os₃(CO)₁₀L (L = bpy, bpm, and dpp)³¹ were prepared by following published procedures. Clusters **1**, **4**, and **5** have been described previously.^{36,37}

The clusters **1–5** were synthesized using a modified procedure: Os₃(CO)₁₀(CH₃CN)₂³⁷ and 1.5 equiv of ligand were stirred in THF at room temperature *in the dark*. When most of the starting material had been consumed, the solvent was evaporated and the product was purified by column chromatography over silica using hexane/THF mixtures *under the exclusion of light*. Clusters **4** and **5** were recrystallized from hexane after chromatography. All complexes were characterized by IR ($\nu(\text{CO})$ in cm⁻¹; in pyridine), ¹H NMR (δ in ppm; in pyridine-*d*₅; see numbering scheme below), UV–vis (λ_{max} in nm (ϵ_{max} in M⁻¹·cm⁻¹), and mass (M⁺ found (calculated)) spectrometry.

Os₃(CO)₁₀(ⁱPr-PyCa) (1). IR: 2084 m, 2034 s, 2002 s, 1992 s, 1976 s, 1963 sh, 1902 w. ¹H NMR: 9.46 (d, 1H, H₄), 9.11 (s, 1H, N=CH), 8.00 (d, 1H, H₁), 7.57 (dd, 1H, H₂), 7.03 (dd, 1H, H₃), 4.51 (m, 1H, CH(CH₃)₂), 1.23 (d, 3H, CH(CH₃)₂), 1.20 (d, 3H, CH(CH₃)₂). UV–vis: THF, 565 (8675); pyridine, 560 (7855).

Os₃(CO)₁₀(ⁱPr-AcPy) (2). IR: 2082 m, 2029 s, 2001 s, 1990 s, 1975 s, 1962 sh, 1899 w. ¹H NMR: 9.49 (d, 1H, H₄), 8.01 (d, 1H, H₁), 7.65 (dd, 1H, H₂), 7.07 (dd, 1H, H₃), 4.20 (m, 1H, CH(CH₃)₂), 2.45 (s, 3H, =C–CH₃), 1.23 (d, 6H, CH(CH₃)₂). UV–vis: THF, 547 (6320), 505 sh; pyridine, 544 (6185). Anal. Found (calcd): C, 24.0 (23.7); H, 1.62 (1.39); N, 2.79 (2.77). Mass: 1014 (1013.94).

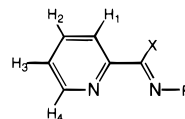
Os₃(CO)₁₀(ⁿPr-AcPy) (3). IR: 2083 m, 2032 s, 1998 s, 1991 s, 1974 s, 1960 sh, 1897 w. ¹H NMR: 9.52 (d, 1H, H₄), 7.94 (d, 1H, H₁), 7.61 (dd, 1H, H₂), 7.09 (dd, H₃), 2.40 (s, 3H, =C–CH₃), 4.31 (m, 1H, =N–CH₂), 4.10 (m, 1H, =N–CH₂), 1.1–1.7 (m, 2H, CH₂), 0.72 (t, 3H, CH₃). UV–vis: THF, 549 (6170); pyridine, 543 (5935). Mass: 1013 (1013.94).

Os₃(CO)₁₀(ⁱPr-DAB) (4). IR: 2093 m, 2045 s, 2010 s, 1992 sh, 1974 sh, 1956 sh, 1906 w. ¹H NMR (253 K): 8.54 (s, 2H, N=CH), 4.51 (m, 2H, =N–CH(CH₃)₂), 1.08 (d, 12H, =N–CH(CH₃)₂). UV–vis: THF, 400 (6505), 439 (6605), 522 (8920); pyridine, 396 (6080), 437 (5835), 522 (7560).

Os₃(CO)₁₀(neoPent-DAB) (5). IR: 2099 m, 2052 s, 2016 s, 1995 sh, 1977 sh, 1954 w, 1903 w. UV–vis: THF, 440 (7385), 524 (6690).

Os₃(CO)₁₀(4,4'-dimethyl-2,2'-bipyridine) was prepared analogous to Os₃(CO)₁₀ (bpy). IR: 2082 m, 2029 s, 1996 sh, 1988 s, 1972 s,

1956 sh, 1893 w. ¹H NMR: 9.20 (d, 2H), 8.21 (s, 2H), 7.03 (dd, 2H), 2.12 (s, 6H). UV–vis (THF): 517 (5565).



Spectroscopic Measurements. UV–vis spectra were recorded on a Varian Cary 4E spectrophotometer, and FTIR spectra on a Bio-Rad FTS-7 or FTS-60A spectrometer. An Oxford Instruments DN 1704/54 liquid-nitrogen cryostat was used for the low-temperature spectroscopic measurements. ¹H NMR spectra were recorded on a Bruker AMX 300 spectrometer, and X-band EPR spectra on a Varian Century E-104A spectrometer. EPR *g*-values were determined relative to the 2,2'-diphenyl-1-picrylhydrazyl (DPPH) radical as an external standard (*g* = 2.0037). Resonance Raman spectra were obtained by excitation of the clusters dispersed in a KNO₃ pellet by one of the lines of a Spectra Physics 2040E argon ion laser and recorded on a Dilor Modular XY system. Field desorption mass spectra were collected on a JEOL JMS SX/SX102A four sector mass spectrometer coupled to a JEOL-MP 7000 data system.

Continuous-Wave Photochemistry. A Spectra Physics 2025 argon ion laser was generally used for the photochemical experiments. The light-sensitive samples (10⁻³–10⁻⁴ M) were prepared in a carefully blinded room, illuminated with red light. Prior to the ¹H NMR detection of the zwitterions formed in pyridine-*d*₅, the solutions of the clusters were irradiated outside the probe using a high-pressure Xe lamp (Oriental AG, 150 mW) with the appropriate cutoff filter. The low-temperature spectra were obtained *in situ* by irradiation into a CIDNP 300 MHz ¹H probe via a glass fiber. The same light source was used for the *in situ* EPR measurements.

Quantum yields of the disappearance of the parent clusters were determined by UV–vis spectroscopy following an automated procedure. The sample solution was kept in a thermostated 1 cm cuvette and irradiated within the spectrophotometer via an optical fiber. The solution was well stirred during the irradiation intervals, and the conversion per interval was kept below 5%. Light intensities were measured with a Coherent 212 power meter which had been calibrated with an Aberchrome 540 solution according to literature procedures.^{38,39} In the computational routine⁴⁰ corrections were made for changes in the partial absorption of the photoactive species caused by both its depletion and by the inner filter effect of the photoproduct(s) formed.⁴¹

For the photoconversion of cluster **3** into its zwitterion **3a** in pyridine the pressure dependence of the quantum yield was studied with a setup described previously.⁴² Samples were irradiated under four different pressures between 0.1 and 150 MPa in a pillbox quartz cell⁴³ which was placed inside a two-window high-pressure cell.⁴⁴ The solutions were stirred by a Teflon-coated magnetic stirrer during irradiation with an Oriol 100 W high-pressure mercury lamp using the appropriate filter (λ = 508 nm). Light intensities were measured by a Si photodiode which was calibrated at 508 nm with Actinochrome N. The incident light was kept in the range (1.3–1.4) × 10⁻⁹ einstein s⁻¹.

Flash Photolysis. Nanosecond time-resolved absorption spectra were obtained by irradiating the sample with 7 ns pulses (fwhm) of a 532 nm line (6 mJ/pulse), obtained by frequency doubling of the 1064 nm fundamental of a Spectra Physics GCR-3 Nd:YAG laser. For photostable systems a 1 cm cuvette was used, and for photolabile

(32) Brunner, H.; Riepl, G.; Benn, R.; Rufinska, A. *J. Organomet. Chem.* **1983**, *253*, 93.

(33) Brunner, H.; Reiter, B.; Riepl, G. *Chem. Ber.* **1984**, *117*, 1330.

(34) Lavery, A.; Nelson, S. M. *J. Chem. Soc., Dalton Trans.* **1985**, 1053.

(35) Bock, H.; tom Dieck, H. *Chem. Ber.* **1967**, *100*, 228.

(36) Zoet, R.; van Koten, G.; Vrieze, K.; Duisenberg, A. J. M.; Spek, A. L. *Inorg. Chim. Acta* **1988**, *148*, 71.

(37) Zoet, R.; Jastrzebski, J. T. B. H.; van Koten, G.; Mahabiersing, T.; Vrieze, K.; Heijdenrijk, D.; Stam, C. H. *Organometallics* **1988**, *7*, 2108.

(38) Heller, H. G.; Langan, J. R. *J. Chem. Soc., Perkin Trans. 2* **1981**, 341.

(39) Aberchromics LTD, S. o. C. a. A. C. College of Cardiff, University of Wales.

(40) Kleverlaan, C. J. *Yield Methode II*; University of Amsterdam: Amsterdam, 1992.

(41) Vichová, J.; Hartl, F.; Vlček, A., Jr. *J. Am. Chem. Soc.* **1992**, *114*, 10903.

(42) Wieland, S.; van Eldik, R.; Crane, D. R.; Ford, P. C. *Inorg. Chem.* **1989**, *28*, 3663.

(43) le Noble, W. J.; Schlott, R. *Rev. Sci. Instrum.* **1976**, *47*, 770.

(44) Fleischmann, F. K.; Conze, E. G.; Stranks, D. R.; Kelm, H. *Rev. Sci. Instrum.* **1974**, *45*, 1427.

samples a homemade flow cell. The probe light from a low-pressure, high-power EG&G FX-504 Xe lamp was passed through the sample cell and dispersed by an Acton SpectraPro-150 spectrograph equipped with a 150 g/mm or 600 g/mm grating and a tunable slit (1–500 μm), resulting in a 6 or 1.2 nm maximal resolution, respectively. The data collection system consisted of a gated intensified CCD detector (Princeton Instruments ICCD-576EMG/RB), a programmable pulse generator (PG-200), and an EG&G Princeton Applied Research Model 9650 digital delay generator. With this OMA-4 setup, I and I_0 are measured simultaneously using a double 8 kernel 200 μm optical fiber. The setup is programmed and accessed using WinSpec (v 1.6.1, Princeton Instruments) under Windows.

Results and Discussion

All complexes possess very similar CO-stretching frequencies and visible absorption bands (see Experimental Section). Just as for the clusters containing an aromatic α -diimine ligand,³¹ the resonance Raman (rR) spectra show that the latter bands belong to Os-to- α -diimine (MLCT) transitions. Thus, the rR spectra of $\text{Os}_3(\text{CO})_{10}(\text{}^i\text{Pr-PyCa})$ (**1**) show strong rR effects for the C=N and C=C stretching modes of the ${}^i\text{Pr-PyCa}$ ligand at 1613, 1539, and 1470 cm^{-1} and weaker effects for a $\nu(\text{CO})$ vibration at 2083 cm^{-1} and for skeletal vibrations at 614, 553, 520, 483, and 438 cm^{-1} . These spectra confirm that the low-energy transition of this cluster involves charge transfer from the metal to the ${}^i\text{Pr-PyCa}$ ligand. According to the rR spectra much less charge is transferred in the case of the cluster $\text{Os}_3(\text{CO})_{10}(\text{neoPent-DAB})$ (**5**). The rR spectra of this cluster show only a very weak rR effect for $\nu_s(\text{CN})$ (1483 cm^{-1}) of the DAB ligand and no rR effect at all for any $\nu(\text{CO})$ vibration. Instead, strong rR effects are observed for DAB-deformation modes at 1146 and 1000 cm^{-1} and for skeletal modes at 629, 595, 519, 473, and 430 cm^{-1} . Hence, the first electronic transition of this cluster has less MLCT and more metal–ligand bonding-to-antibonding character. This observation points to a strong Os–DAB π -back-bonding, which is also evident from the low frequency of $\nu_s(\text{CN})$ (1483 cm^{-1}) of the DAB ligand.

The photoreactions of the clusters were studied in different solvents after irradiation into their visible absorption band. First, the formation of zwitterions in coordinating solvents will be dealt with, and then we will report the formation of biradicals in weakly and noncoordinating solvents as well as their transformation into zwitterions in the presence of a Lewis base.

Zwitterions. In a previous article³¹ it was shown that irradiation of the cluster $\text{Os}_3(\text{CO})_{10}(\text{bpy})$ in acetonitrile or pyridine affords a species, which was identified as the zwitterion ${}^-\text{Os}(\text{CO})_4\text{--Os}(\text{CO})_4\text{--Os}^+(\text{S})(\text{CO})_2(\text{bpy})$, with the use of infrared, resonance Raman, UV–vis absorption, and ${}^1\text{H}$ NMR spectroscopies. Hereinafter we present additional information about the formation and properties of these zwitterions in the case of clusters **1–5**.

Zwitterion formation not only is determined by the coordinating ability of the solvent but it also depends on the π -accepting properties of the α -diimine ligand. Clusters **1–3**, all containing closely related α -diimine ligands with pyridine and imine groups, produce zwitterions at room temperature in DMSO, nitriles R-CN (R = Me, Et, nPr), pyridine, 2-picoline, or pyridazine. Most zwitterions are transient species and mainly regenerate their parent cluster. In less coordinating solvents such as THF, acetone, and 2-MeTHF, zwitterions are only formed at lower temperatures. They are stable species in THF and acetone at 183 K and in a 2-MeTHF glass at 133 K.

In contrast to **1–3**, the R-DAB clusters **4** and **5** do not form zwitterions at room temperature. The zwitterion **4a** was

Table 1. IR Data ($\nu(\text{CO})$ in cm^{-1}) for the Zwitterions **1a–5a** in Pyridine (at 293 K Unless Stated Otherwise)

1a	2073 w	1992 vs	1970 vs	1930 w	1898 w	1874 m
2a	2071 w	1988 vs	1968 vs	1925 w	1898 w	1873 m
3a	2070 w	1988 vs	1966 vs	1927 w	1891 w	1871 m
4a^d	2077 vw	1996 vs	1973 vs	1937 w	1903 w	1878 m
5a^d	2077 vw	1997 vs	1976 vs	1938 w	1910 w	1882 m

^a Measured at 253 K.

Table 2. Maxima of the Lowest-Energy Absorption Bands (in nm) of the Zwitterions in Various Solvents, with the Absorption Maxima of the Parent Clusters in Parentheses^{a,b}

zwitterion	pyridine, 263 K ^d	butyronitrile, 223 K	THF, 183 K
1a	573 (556)	525 (547)	553 (544)
2a	566 (539)	515 (530)	535 (529)
3a	561 (541)	509 (535)	529 (532)
4a	571 (524)	no zw ion	no zw ion
L = bpy ^c	537 (521)	497 (517)	513 (515)
L = bpym ^c	588 (551)	536 (541)	559 (532)
L = dpp ^c	610 (568)	561 (561)	578 (550)

^a The UV–vis spectrum of **5a** could not be measured accurately due to its limited thermal stability. ^b Extinction coefficients of the clusters **1–4** are presented in the Experimental Section. ^c Data for the zwitterions ${}^-\text{Os}(\text{CO})_4\text{--Os}(\text{CO})_4\text{--Os}^+(\text{S})(\text{CO})_2(\text{L})$ and their parent clusters. ^d Extinction coefficients ($\text{M}^{-1}\cdot\text{cm}^{-1}$) at λ_{max} of **1a–4a** at 263 K in pyridine: **1a**, 6100; **2a**, 5120; **3a**, 4800; **4a**, 7040.

Table 3. ${}^1\text{H}$ NMR Data for the Zwitterions **1a–4a^a** (δ in ppm, in pyridine- d_5)

zw ion	H4	H1	H2	H3	X group	R group
1a	9.04 d	8.22 d	7.76 dd	<i>b</i>	9.69 s	4.64 (m, 1H) 1.14 (d, 3H)
2a	9.03 d	8.30 d	7.84 dd	7.43 dd	2.66 s	4.60 (m, 1H) 1.21 (d, 3H) 0.85 (d, 3H)
3a	9.07 d	8.23 d	7.94 dd	7.43 dd ^b	2.55 s	0.52 (t, CH ₃) ^c
4a					9.38 s	4.40 (m, 2H) 1.00 (d, 6H) 0.59 (d, 6H)

^a The ${}^1\text{H}$ -NMR spectrum of **5a** could not be measured accurately due to its limited thermal stability. ^b Obscured by solvent resonance. ^c Propyl CH₂ resonances largely coinciding with parent cluster signal.

produced in butyronitrile at 223 K and at 253 K in pyridine and DMSO, while **5a** was obtained at 253 K only in the latter solvents.

The CO-stretching frequencies of the zwitterions **1a–5a** in pyridine are collected in Table 1. For selected clusters the maxima of their MLCT bands in pyridine, butyronitrile, and THF at low temperatures are presented in Table 2, together with those of the zwitterions containing the aromatic α -diimine ligands 2,2'-bipyridine (bpy), 2,2'-bipyrimidine (bpym), and 2,3-dipyrid-2-ylpyrazine (dpp), respectively. The MLCT maxima are slightly shifted and broadened with respect to those of the parent clusters, and their ϵ_{max} values are 20–40% lower.

The ${}^1\text{H}$ NMR spectra of the zwitterions were measured in deuterated pyridine, because of their long lifetimes in this solvent. The high-quality spectra confirm the diamagnetic nature of the photoproducts, and the observed shifts agree with the charge separation in these systems. Thus, most proton signals of the α -diimine ligands are shifted to higher ppm values relative to those of the parent cluster (Table 3). The shifts are, however, rather small since σ donation by the coordinated pyridine partly compensates the increase of positive charge at the metal– α -diimine fragment. In contrast to this, a remarkable shift of ca. 0.4 to lower ppm values is observed for the *ortho*-

Table 4. Lifetimes of the Zwitterions in Acetonitrile and of the Biradical Transients in THF^a in Nanoseconds (Estimated Error 5%; 9% for **3** in THF) at Room Temperature (Numbers in Parentheses Taken from Ref 31)

cluster	acetonitrile	THF
Os ₃ (CO) ₁₀ (bpy)	(5.6 ± 0.1) × 10 ⁹	299 (246)
Os ₃ (CO) ₁₀ (bpym)	(9.0 ± 0.1) × 10 ⁹	455 (568)
Os ₃ (CO) ₁₀ (dpp)	(10.8 ± 0.2) × 10 ⁹	1007 (914)
1	(102 ± 5) × 10 ⁹	204
2	(38 ± 1) × 10 ⁹	111
3	(29 ± 1) × 10 ⁹	72

^a In toluene and 2-chlorobutane no transients were observed except for **2**: $\tau = ca. 26$ ns (2-chlorobutane); $\tau = ca. 5$ ns (toluene).

proton H4 of the pyridine ring of **1a–3a**, suggesting that this proton is in close contact with the Os(CO)₄[−] fragment of the zwitterion. This effect may also be responsible for the rather efficient *ortho*-metalation reaction of cluster **1**.³⁶ The substituents R of the R-PyCa and R-AcPy ligands show an increased asymmetry in the zwitterions. The ¹H NMR signals of the two methyl groups of the ⁱPr substituent of **1a** and **2a** differ by ca. 0.3 ppm, whereas they nearly coincide for **1** and **2**. This effect may be due to the coordination of pyridine in the zwitterion. According to the ¹H NMR spectra, the imine protons of the R-DAB zwitterions **4a** and **5a** are equivalent and their resonances are shifted by 0.85 to higher ppm values with respect to those of the parent clusters. Just as for **1a**, the methyl protons of the ⁱPr groups of **4a** give two doublets which are 0.4 ppm apart.

Lifetimes and (Pressure-Dependent) Quantum Yields. In agreement with our previous observations on related clusters³¹ both the formation and the lifetimes of the zwitterions strongly depend on the coordinating ability of the solvent. In nitrile solvents, **1a–3a** live seconds; in pyridine, 2-picoline, pyridazine, and DMSO they have a lifetime of several minutes. The latter lifetimes could not be determined accurately, since the zwitterions slowly decompose in these solvents. The zwitterions could even be stabilized completely by adding a salt such as (tBu)₄NBr to the solution. Thus, regeneration of the parent cluster by reaction between the Os(CO)₄[−] and Os⁺(S)(CO)₂(α -diimine) fragments of the zwitterion is hampered by the solvent or anion S. A similar behavior has been observed for Mn(CO)₃(Pr-DAB)[−] and Mn(X)(CO)₃(Pr-DAB)⁰⁺, which react rapidly with each other to give [(Mn(CO)₃(Pr-DAB))₂] for X = THF, more slowly for X = CH₃CN, and very slowly for X = Br[−].⁴⁵ Similarly, the ions Mn(CO)₅[−] and Mn(S)(CO)₃(α -diimine)⁺, produced by irradiation of (CO)₅MnMn(CO)₃(α -diimine), are stable in THF at sufficiently low temperatures but regenerate the parent complex on raising the temperature.^{8,13,29}

According to the data in Table 4, the zwitterions **1a–3a** live longer in acetonitrile than those containing an aromatic α -diimine ligand. This effect is caused by the stronger σ -donating and weaker π -accepting properties of the latter ligands. They donate more negative charge to the metal, and as a result, their zwitterions have weaker metal–solvent bonds and shorter lifetimes.

Quantum yields (Φ) for the disappearance of the clusters on zwitterion formation were determined for **1–3** in pyridine in the temperature range of 253–278 K in which **1a–3a** are stable. For cluster **4** the corresponding quantum yield was determined at 253 K since **4a** is thermally unstable in pyridine at higher temperatures. The temperature dependence of Φ was also

Table 5. Quantum Yields $10^2\Phi(T)$,^a Activation Energies E_a , and Preexponential Factors Φ_0 of the Photochemical Zwitterion Formation in Pyridine for Clusters **1–4** (T in K, λ_{irr} in nm, E_a in cm^{−1})

cluster	1	2^b	3	4		
λ_{irr}	514.5	457.9	488.0	514.5	514.5	
$10^2\Phi(278)$	19.7	34.2		32.3	21.3	
$10^2\Phi(268)$	17.7	30.6		30.1	19.2	
$10^2\Phi(263)$	16.2	29.2	28.3	28.2	18.3	
$10^2\Phi(253)$	13.7	26.3		25.9	15.1	10.9
E_a	718	511		440	689	
Φ_0	8.2	4.8		3.2	7.7	

^a $T \pm 0.1$ K; estimated relative error approximately 3%. ^b $10^2\Phi$ for **2** in 2-picoline ($\lambda_{exc} = 514.5$ nm): 29.0 (243 K), 30.8 (248 K), 34.2 (258 K), and 36.0 (263 K); $E_a = 477$ cm^{−1}; $\Phi_0 = 4.9$.

determined; for **2** this was done at two irradiation wavelengths within the visible absorption band. From these data the activation energy E_a and the preexponential factor Φ_0 were determined with the Arrhenius-type equation $\Phi = \Phi_0 \exp(-E_a/RT)$ (Table 5). The values of Φ are rather high and temperature dependent, but there is virtually no dependence on the wavelength of irradiation. The α -diimine ligands of **1–3** have very similar electronic properties, but the ⁱPr-AcPy ligand of **2** is sterically most demanding. This steric effect apparently lowers E_a and increases Φ , although the effect on Φ is partly offset by a decrease of Φ_0 , i.e. by an increase of the nonproductive decay to the ground state. An increase of the bulkiness of the solvent molecules by using 2-methylpyridine (2-picoline) instead of pyridine had no influence on Φ .

To obtain more information about the character of the primary photoprocess of the zwitterion formation, the dependence of Φ on applied pressure was studied for **3** in pyridine. The value of Φ decreased with increasing pressure: from 0.216 at $P = 0.1$ MPa to 0.179 (50 MPa), to 0.155 (100 MPa), and to 0.137 (150 MPa). The apparent volume of activation,^{42,46–53} ΔV^\ddagger , was obtained from the slope of the linear plot of $\ln[\Phi/(1 - \Phi)]$ vs pressure. Values obtained from such plots are preferred over those of $\ln \Phi$ vs pressure since they represent the difference between the volume of activation of the reaction and that of the nonradiative excited-state decay.⁴⁷ The correlation coefficient was 0.932, and $\Delta V^\ddagger = +7.0 \pm 0.5$ cm³·mol^{−1}. The small positive value of ΔV^\ddagger is rather surprising since zwitterion formation as well as the coordination of a solvent molecule are expected to be accompanied by a significant volume collapse due to increased electrostriction and a decreased intrinsic volume, respectively. The positive value indicates that the volume change, and thus the barrier for the zwitterion formation, are governed by *bond cleavage*, which is partly offset by the increase of electrostriction and by the coordination of pyridine.

Biradicals. As shown above, zwitterions are formed at room temperature in DMSO and in N-donor solvents such as acetonitrile or pyridine; no zwitterions were obtained by irradiation in weakly or noncoordinating solvents such as THF or toluene. However, even in such media a rather inefficient photoreaction occurs for clusters **1**, **4**, and **5** and not for **2** and **3**. All three clusters produce an analogous stable photoproduct⁵⁴

(46) van Eldik, R.; Merbach, A. E. *Comments Inorg. Chem.* **1992**, *12*, 341.

(47) Skibsted, L. H.; Weber, W.; van Eldik, R.; Kelm, H.; Ford, P. C. *Inorg. Chem.* **1983**, *22*, 541.

(48) van Eldik, R.; Asano, T.; le Noble, W. J. *Chem. Rev.* **1989**, *89*, 549.

(49) Wieland, S.; van Eldik, R. *Coord. Chem. Rev.* **1990**, *97*, 155.

(50) Schneider, K. J.; van Eldik, R. *Organometallics* **1990**, *9*, 1235.

(51) Wieland, S.; Bal Reddy, K.; van Eldik, R. *Organometallics* **1990**, *9*, 1802.

(52) Fu, W. F.; van Eldik, R. *Inorg. Chim. Acta* **1996**, *251*, 341.

(53) Fu, W. F.; van Eldik, R. *Organometallics* **1997**, *16*, 572.

(45) Rossenaar, B. D.; Hartl, F.; Stufkens, D. J.; Amatore, C.; Maisonhaute, E.; Verpeaux, J.-N. *Organometallics* **1997**, *16*, 4675.

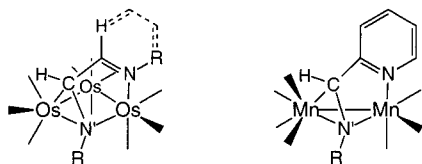


Figure 2. Schematic structures of the isomeric photoproduct $\text{Os}_3(\text{CO})_{10}(\sigma\text{-N},\mu_2\text{-N}',\eta^2\text{-C}=\text{N}'\text{-L})$ ($\text{L} = \text{R-DAB}$ or R-PyCa) (left) and of $(\text{CO})_4\text{Mn}(\sigma\text{-N},\mu_2\text{-N}',\eta^2\text{-C}=\text{N}'\text{-R-PyCa})\text{Mn}(\text{CO})_3$ (right).

with CO-stretching frequencies which are nearly identical with those reported by Zoet *et al.*^{36,37} for the clusters $\text{Os}_3(\text{CO})_{10}(\sigma\text{-N},\mu_2\text{-N}',\eta^2\text{-C}=\text{N}'\text{-}\alpha\text{-diimine})$ (2088 m, 2051 vs, 2026 m, 2007 m, 1986 m, 1975 m, 1967 w, 1945 w cm^{-1} for the product of **1** in toluene; Zoet *et al.* obtained 2086, 2049, 2026, 2008, 1987, 1977, 1969, and 1951 cm^{-1} for the ⁱPr-PyCa product in hexane). These α -diimine-bridged clusters were prepared by Zoet *et al.*^{36,37} by the thermal reaction of $\text{Os}_3(\text{CO})_{10}(\text{CH}_3\text{CN})_2$ with the appropriate R-PyCa or R-DAB ligand. The structure, which is schematically depicted in Figure 2, was established by X-ray diffraction for the cyclopropyl-DAB cluster. In this product one Os–Os bond is broken, the α -diimine ligand has changed its coordination from $\sigma\text{-N},\text{N}'(4e)$ into $\sigma\text{-N},\mu_2\text{-N}',\eta^2\text{-C}=\text{N}'(6e)$, and, to compensate for this change of coordination, a carbonyl ligand has been transferred from one Os atom to another. The lifting of the conjugation within the α -diimine ligand results in the disappearance of the MLCT band at ca. 580 nm and a concomitant slight increase of absorption in the 300–400 nm region. This isomerization reaction is not observed for the clusters **2** and **3**; the methyl substituent at the imine carbon atom apparently prevents the π -coordination of the R-AcPy ligands.

Figure 2 shows for comparison the schematic structure of the complex $(\text{CO})_4\text{Mn}(\sigma\text{-N},\mu_2\text{-N}',\eta^2\text{-C}=\text{N}'\text{-R-PyCa})\text{Mn}(\text{CO})_3$, which has been determined by X-ray diffraction for $\text{R} = \text{}^i\text{Pr}$.¹² This complex was formed in very viscous media (paraffin) by reaction of the $\text{}^*\text{Mn}(\text{CO})_5$ and $\text{Mn}(\text{CO})_3(\text{R-PyCa})^*$ radicals. The α -diimine ligand bridges in the same way as for the Os clusters, but a carbonyl ligand is released instead of transferred and the metal–metal bond is re-formed. Despite their different structures, both the Os and Mn products are most probably formed via the same mechanism, i.e. by the radical coupling reaction depicted for the Mn complexes in Scheme 1. This points to the formation of biradicals of the type $\text{}^*\text{Os}(\text{CO})_4\text{-Os}(\text{CO})_4\text{-Os}(\text{CO})_2(\alpha\text{-diimine})^*$ as primary photoproducts of the $\text{Os}_3(\text{CO})_{10}$ -(α -diimine) clusters in weakly and noncoordinating solvents. The reaction is not efficient; for cluster **1** the quantum yield is ca. 0.003 in THF and 0.002 in toluene.

In agreement with the radical mechanism of the isomer formation, the reaction was completely quenched when a 100-fold excess of nitrosodurene or CCl_4 was added to the solution. The biradicals could also be detected and characterized by nanosecond time-resolved absorption spectroscopy, and their adducts with nitrosodurene could be observed with EPR spectroscopy.

EPR Spectra. On irradiation of the clusters **1–5** and $\text{Os}_3(\text{CO})_{10}(\text{bpy}')$ in toluene or THF in the presence of excess nitrosodurene, spin-trapped radicals were observed which slowly decayed at room temperature but remained stable at $T \leq 273$ K. Representative spectra, recorded on irradiation of **4** and of $\text{Os}_3(\text{CO})_{10}(\text{}^i\text{Pr-PyCa})^{55}$ in toluene, are shown in Figure 3a,c, respectively. These spectra apparently belong to tumbling anisotropic species since they exhibit temperature-dependent broadening of the lines with increasing magnetic field strength,

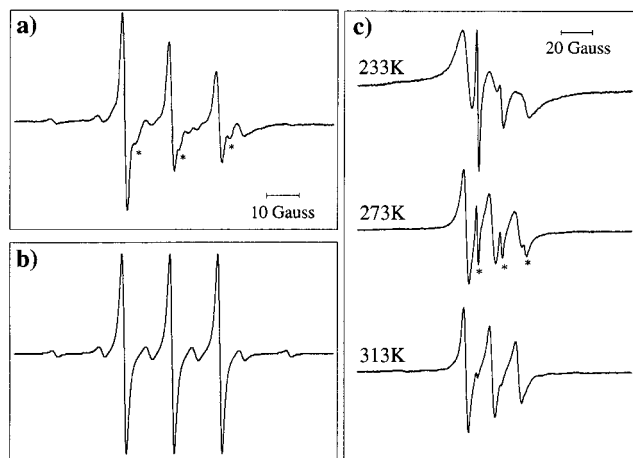


Figure 3. EPR spectra of the nitrosodurene-trapped radicals produced on irradiation of solutions in toluene (a) of $\text{Os}_3(\text{CO})_{10}(\text{}^i\text{Pr-DAB})$ (**4**) with (b) the simulated isotropic spectrum and (c) of $\text{Os}_3(\text{CO})_{10}(\text{}^i\text{Pr-PyCa})^{55}$ at variable temperatures. Asterisks indicate lines due to another spin-trapped radical.

characteristic for an anisotropic g -tensor and a nuclear–electronic hyperfine-tensor effect (motional modulations).⁵⁶

The formation of spin adducts with nitrosodurene is evident from the typically “high” g -values of 2.0068 for **3** and 2.0078 for **4** and by the hyperfine splitting (hfs) found for one ^{14}N nucleus ($I = 1$, 99.63%), $a_{\text{N}} = 15.0 \pm 0.2$ G. These data correspond with a localization of the odd electron in the low-lying $\pi^*\text{NO}$ orbital of the spin trap.^{57,58} The EPR spectrum of Figure 3a also shows additional hfs due to one ^{189}Os nucleus ($I = 1.5$, 16.1%), $a_{\text{Os}} = 14.4 \pm 0.2$ G (with a little variation between the different adducts). This hfs is a characteristic feature of most EPR spectra, but it is not clearly resolved in Figure 3c due to larger line widths. The hfs of the low-abundance ^{187}Os nucleus ($I = 0.5$, 1.6%) could not be detected. In essence, only one odd electron in the biradical can be trapped by nitrosodurene, most likely the one that initially resides on the coordinatively unsaturated $\text{Os}^+(\text{CO})_2(\alpha\text{-diimine})^*$ moiety. Most EPR spectra show similar signals of a second spin adduct at slightly smaller g -values (marked with an asterisk), which become more apparent at low temperatures (Figure 3c). Cluster **1** shows a more complicated pattern in toluene. No biradicals are trapped in pyridine either because they are not formed or since they are instantaneously transformed into zwitterions.

Nanosecond Time-Resolved Absorption Spectra. Nanosecond time-resolved spectra were obtained by irradiation of **1–3** in THF, 2-Cl-butane, and toluene with the 532 nm line of a Nd:YAG laser. Figure 4 shows the difference absorption spectra of **2** in THF at $t = 30\text{–}390$ ns after the pulse with a delay of 10 ns between the first 12 spectra. There is a strong bleach at about 540 nm which nearly coincides with the ground-state absorption. The transient species absorbs in the whole spectral region and has a lifetime of 111 ± 5 ns, measured at five wavelengths. In agreement with our observation that **2** does not produce a long-lived photoproduct in THF (isomer formation cannot occur for this cluster; vide supra), there is nearly

(55) The ⁱPr-PyCa derivative of **1** was found to be the most suitable candidate for the EPR study at variable temperatures. The corresponding EPR spectra are therefore presented here, although the synthesis and photochemistry of this cluster (mostly resembling that of **1**) will be described in a forthcoming article.

(56) Mabbs, F. E. *Chem. Soc. Rev.* **1993**, 313 and references therein.

(57) Kleverlaan, C. J. To be published.

(58) Andr a, R. R.; de Lange, W. G. J.; van der Graaf, T.; Rijkhoff, M.; Stufkens, D. J.; Oskam, A. *Organometallics* **1988**, *7*, 1100.

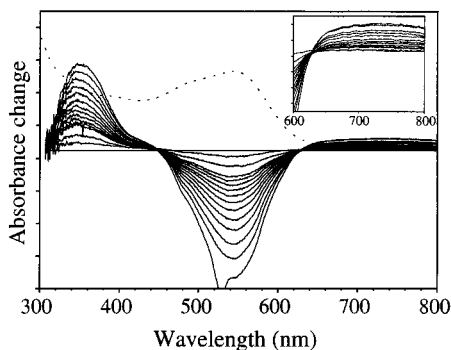


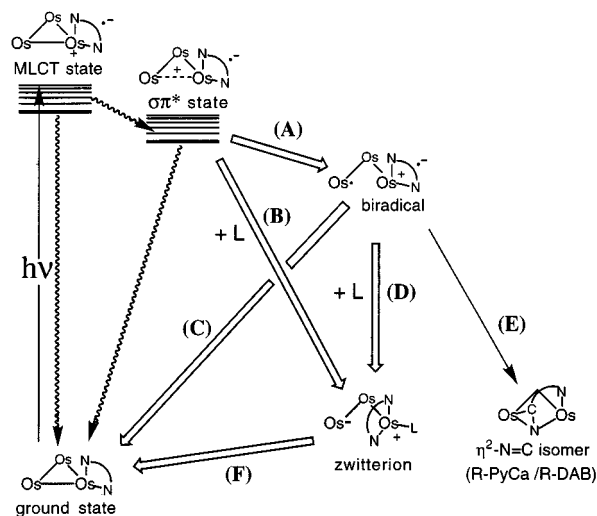
Figure 4. Nanosecond transient absorption spectra of Os₃(CO)₁₀(ⁱPr-AcPy) (**2**) in THF at 298 K. The time delay between the first 12 spectra is 10 ns; after that it is 30 ns. The dotted curve represents the ground-state absorption spectrum of the cluster in THF.

complete recovery of this cluster. The short lifetime of the transient does not agree with that of a zwitterion, and the transient spectrum deviates appreciably from that of zwitterion **2a** in THF at 183 K (Table 2).

Thus, the transient species is not a zwitterion but either an excited state or a biradical. In such a biradical one radical is the •Os(CO)₄ group, the other one the Os⁺(CO)₂(ⁱPr-AcPy⁻) radical fragment. The assignment to a biradical is supported by the presence of a very broad transient absorption above 600 nm, which is rather specific for complexes in metal-to-α-diimine excited states^{15,28,59–61} and for α-diimine radical anions containing at least one aromatic group.^{62,63} The assignment to a biradical is supported by the observation that the lifetime of the transient significantly increases by the uptake of a solvent molecule by the Os⁺(CO)₂(ⁱPr-AcPy⁻) radical fragment.^{64,65} Thus, in the case of **2** the lifetime of the transient increases from ca. 5 ns in toluene to 26 ns in 2-Cl-butane and to 111 ns in THF. If the transient species were instead an excited state, its lifetime would have been shortest in THF.

As the lifetimes of the biradicals are much shorter and the quantum yields of their formation are much lower in toluene and 2-Cl-butane than in THF, these lifetimes are less accurate in the former solvents. The low quantum yields agree with the inefficient formation of the isomers⁵⁴ in noncoordinating solvents; the short lifetimes explain why the biradicals are only trapped if a large excess of nitrosodurene or CCl₄ is added to the solution. As expected, the lifetime of the biradical increases with decreasing energy of the lowest π* orbital of the α-diimine, at least for closely related clusters. Thus, in the order from bpy to bpm to dpp, the π* orbital decreases in energy and the lifetime of the biradical increases from 255 to 568 to 914 ns (Table 4). Finally, the biradicals are clearly primary photoproducts since picosecond transient absorption measurements of Os₃(CO)₁₀(bpy) in THF have shown³¹ that they are present directly after the 30 ps laser pulse and during the next 10 ns.

Scheme 2. Proposed Mechanism for the Photoreactions of the Clusters Os₃(CO)₁₀(α-diimine)^a



^a The separate reaction steps (A)–(F) depend on the solvent used: (i) (A) + (C) and (A) + (E) in toluene, 2-chlorobutane, and THF; (ii) (B) + (F) and/or (A) + (D) + (F) in acetonitrile, pyridine, and THF/2-MeTHF at low temperature; (iii) (A) + (D) + (F) in THF + 0.5 M CH₃CN.

Conversion of Biradicals into Zwitterions. The radicals formed by irradiation of the binuclear complexes (CO)₅MnMn(CO)₃(α-diimine) in an apolar solvent transform into ions when a Lewis base is added to the solution (Scheme 1).^{8,29} To establish a similar reaction for the clusters under study, a large excess of acetonitrile (0.5 M) was added to a solution of cluster **2** in THF. The nanosecond transient absorption spectra of this solution, recorded directly after the laser pulse, show the characteristic long-wavelength absorption of the biradical, which gradually transforms into a new band with an apparent maximum at ca. 650 nm. At the same time the bleach does not disappear completely; at 300 ns after the pulse it has decreased to about 45% of its initial value and shifted slightly to shorter wavelength. This difference spectrum, which does not change during the next 10 μs, represents the spectral change accompanying the conversion of **2** into its zwitterion **2a** stabilized by acetonitrile. This is confirmed by comparing the final spectrum with that obtained for **2** in neat acetonitrile. The conversion of the biradicals into zwitterions is not complete since the bleach decreases to 45% of the initial value, whereas a decrease to ca. 30% is expected in view of the ε_{max} values of the cluster and its zwitterion (compare Experimental Section and Table 2). This reaction of the biradicals in THF/0.5 M CH₃CN only occurs for **1–3** and not for **4** and **5**, as the latter clusters do also not produce zwitterions in neat acetonitrile at room temperature (vide supra).

Mechanistic Aspects. The photochemical reactions discussed in the preceding sections are initiated by irradiation into the low-energy MLCT transitions. Normally such an MLCT state is not reactive but it may cross to a reactive (e.g. LF) state from which the reaction occurs. According to the nanosecond and picosecond³¹ experiments biradical formation, i.e. homolysis of a metal–metal bond, is a primary photoprocess of these clusters just as for the binuclear metal–metal-bonded complexes described in the Introduction.^{1–17} In analogy with these binuclear complexes, biradical formation of the clusters is assumed to occur from a ³σπ* state, after surface crossing from the optically accessible MLCT state(s) (Scheme 2). There is most likely no overlap between the σ orbital of the Os₃ core^{66,67}

(59) Nieuwenhuis, H. A.; Stufkens, D. J.; McNicholl, R. A.; Al-Obaidi, A. H. R.; Coates, C. G.; Bell, S. E. J.; McGarvey, J. J.; Westwell, J.; George, M. W.; Turner, J. J. *J. Am. Chem. Soc.* **1995**, *117*, 5579.

(60) Rossenaar, B. D.; Stufkens, D. J.; Vlček, A., Jr. *Inorg. Chem.* **1996**, *35*, 2902.

(61) Rossenaar, B. D.; Stufkens, D. J.; Vlček, A., Jr. *Inorg. Chim. Acta* **1996**, *247*, 247.

(62) Klein, A.; Kaim, W. *Organometallics* **1995**, *14*, 1176.

(63) van Dijk, H. K.; Servaas, P. C.; Stufkens, D. J.; Oskam, A. *Inorg. Chim. Acta* **1985**, *104*, 179.

(64) van Outersterp, J. W. M.; Hartl, F.; Stufkens, D. J. *Organometallics* **1995**, *14*, 3303.

(65) Stor, G. J.; Hartl, F.; van Outersterp, J. W. M.; Stufkens, D. J. *Organometallics* **1995**, *14*, 1115.

and the π^* orbital of the α -diimine by which the $\sigma \rightarrow \pi^*$ transition becomes allowed. The rR spectra show that the latter transition can indeed only be a minor contributor to the visible absorption band.

According to the transient absorption spectra and the quantum yields of isomer formation, the homolysis reaction is more efficient in THF than in toluene. There is apparently a solvent-dependent barrier for the homolytic cleavage of an Os–Os bond. A similar activation energy (E_a) was derived from the quantum yield data for the conversion of **2** into the zwitterion **2a** in pyridine. Its value does not depend on the energy of excitation, which means that the barrier does not exist between the optically populated MLCT state(s) and the reactive $^3\sigma\pi^*$ state. Instead, E_a represents an activation energy for the zwitterion formation from the latter state. This result is in agreement with the pressure-dependent quantum yield data which show that the transition state of the rate-determining step involves coordination of a solvent molecule. On the other hand, these data also reveal that the zwitterion formation must have a large dissociative contribution since the overall activation volume is positive. It is therefore not clear at which stage during the homolysis reaction from the $^3\sigma\pi^*$ state the solvent molecules preferably coordinate and induce the charge shift leading to the zwitterion formation. Both pathways, (B) and (A) + (D), of Scheme 2 are therefore possible, although pathway (B) is preferred for the clusters **1–3** in pyridine since no intermediate biradicals could be trapped in this solvent. Pathway (A) + (D) will e.g. be followed on irradiation of the clusters in THF/0.5 M CH_3CN . In this case irradiation of the cluster gives rise to biradical formation from the $^3\sigma\pi^*$ state. The coordinatively unsaturated $\text{Os}^+(\text{CO})_2(\alpha\text{-diimine}^{\bullet-})$ fragment of the biradical takes up a THF molecule, which is then replaced by a CH_3CN molecule. This induces an unbalance of charge and initiates an intramolecular electron transfer to the $\bullet\text{Os}(\text{CO})_4$ radical. Such a reaction is quite common for binuclear complexes such as $(\text{CO})_5\text{MnMn}(\text{CO})_3(\alpha\text{-diimine})$.¹³ The radicals $\text{Mn}^+(\text{CO})_3(\alpha\text{-diimine}^{\bullet-})$, formed by irradiation of these complexes, take up a strongly coordinating solvent molecule (S) and react with the $\bullet\text{Mn}(\text{CO})_5$ radicals or with the parent complex to give the ions $\text{Mn}(\text{CO})_5^-$ and

$\text{Mn}^+(\text{S})(\text{CO})_3(\alpha\text{-diimine})$. The varying behavior of the clusters in THF, viz. the formation of biradicals and isomers at room temperature and of zwitterions at low temperatures, is also in line with the photochemistry of the Mn–Mn-bonded complexes, viz. production of the dimers $\text{Mn}_2(\text{CO})_{10}$ and $[\text{Mn}(\text{CO})_3(\alpha\text{-diimine})]_2$ at room temperature and of the photodisproportionation products $\text{Mn}(\text{CO})_5^-$ and $\text{Mn}(\text{S})(\text{CO})_3(\alpha\text{-diimine})^+$ below 200 K.

Both the biradicals and the zwitterions regenerate the parent cluster, although a small part of the biradicals reacts further to give an α -diimine-bridged isomer in the case of the R-PyCa and R-DAB clusters. Both back-reactions to the parent cluster are retarded by the coordination of solvent molecules.

Conclusions

The results of this study clearly show that the photochemical behavior of these clusters is very similar to that of the corresponding binuclear metal–metal-bonded complexes. However, the clusters retain a trinuclear conformation in their primary photoproduct, and secondary thermal reactions are therefore intramolecular, whereas they are all intermolecular for the binuclear analogues. Both the biradicals and zwitterions have two close-lying reactive sites. Work is in progress to study the reactivity of these sites with respect to olefins and other small molecules.

Acknowledgment. Prof. Dr. A. Oskam is thanked for his continued interest and support. Dr. C. J. Kleverlaan is thanked for his assistance with the rapid scan FT-IR and EPR experiments, and Th. L. Snoeck and J. van Ramesdonk are thanked for help with the Raman and the time-resolved absorption experiments, respectively. The Netherlands Foundation for Chemical Research (SON) and The Netherlands Organization for the Advancement of Pure Research (NWO) are thanked for their financial support.

Supporting Information Available: Figure 5, showing resonance Raman spectra ($\lambda_{\text{exc}} = 514.5 \text{ nm}$) of **1** and **5** in a KNO_3 pellet, Figure 6, showing infrared and UV–vis spectral changes accompanying the formation of zwitterion **1a** by irradiation of **1** in pyridine, and Figure 7, showing transient spectra of **2** in THF/0.5 M CH_3CN (3 pages). Ordering information is given on any current masthead page.

IC9707319

(66) Tyler, D. R.; Levenson, R. A.; Gray, H. B. *J. Am. Chem. Soc.* **1978**, *100*, 7888.

(67) Delley, B.; Manning, M. C.; Ellis, D. E.; Berkowitz, J.; Troglor, W. C. *Inorg. Chem.* **1982**, *21*, 2247.